Calculation of the Microscopic and Macroscopic Linear and Nonlinear Optical Properties of Liquid Acetonitrile. II. Local Fields and Linear and Nonlinear Susceptibilities in Quadrupolar Approximation

A. Avramopoulos, M. G. Papadopoulos, and H. Reis*

Institute of Organic and Pharmaceutical Chemistry, National Hellenic Research Foundation, Vasileos Constadinou 48, Athens, Greece

Received: October 9, 2006; In Final Form: December 21, 2006

A discrete model based on the multipolar expansion including terms up to hexadecapoles was employed to describe the electrostatic interactions in liquid acetonitrile. Liquid structures obtained form molecular dynamics simulations with different classical, nonpolarizable potentials were used to analyze the electrostatic interactions. The computed average local field was employed for the determination of the environmental effects on the linear and nonlinear electrical molecular properties. Dipole−dipole interactions yield the dominant contribution to the local field, whereas higher multipolar contributions are small but not negligible. Using the effective in-phase properties, macroscopic linear and nonlinear susceptibilities of the liquid were computed. Depending on the partial charges describing the Coulomb interactions of the force field employed, either the linear properties (refractive index and dielectric constant) were reproduced in good agreement with experiment or the nonlinear properties [third-harmonic generation (THG) and electric field induced second-harmonic (EFISH) generation] and the bulk density but never both sets of properties together. It is concluded that the partial charges of the force fields investigated are not suitable for reliable dielectric properties. New methods are probably necessary for the determination of partial charges, which should take into account the collective and long-range nature of electrostatic interactions more precisely.

1. Introduction

It is well-established that intermolecular interactions have a significant effect on the nonlinear optical (NLO) properties measured in the liquid phase.[1] Thus, there is a great need for the development of theoretical models appropriate for the description of the environmental effects on the NLO properties, considering that most of the measurements on highly polar NLO molecules are performed in solutions. Several such methods have been proposed,[2,3] generally in the framework of continuum solvation models, with their inherent limitations. However, the proper description of the intermolecular interactions in solutions still remains a challenging task.[4] This is a problem of considerable importance, when one tries to approximate the NLO properties resulting from experiments like dc electric field second-harmonic (EFISH) generation.[5] Polar, aprotic liquid systems are associated with remarkable environmental effects, which subsequently affect the magnitude of the NLO molecular properties.[6] In such liquids, one may expect that the local field created by molecular interactions constitutes the main effect of the environment on the molecular electric properties.

In the first part of this series, we investigated the predictions of a continuum model in the form of the simple Onsager−Lorentz local field description for the linear and nonlinear optical properties of liquid acetonitrile.[7] It was found that this model is in good agreement with experimental results. However, there is experimental evidence which points to the existence of local structure in polar, aprotic liquids.[8,9] Effects of this kind of ordering on dielectric properties would not be taken into account by a pure continuum model as the Onsager−Lorentz local field model. Thus, in order to go beyond the continuum models, and to investigate the effect of the environment on the NLO molecular properties in a discrete description, we employed in this work an approach which combines molecular dynamics with a discrete local field (DLF) model to liquid acetonitrile. In this approach, molecular dynamics simulations are employed to create liquid structure information in the form of trajectories, which are subsequently analyzed using an induction model based on multipole expansions of the molecular charge densities. Due to the separation of the two computational steps, it is possible to use high-level ab initio methods in the second step, which in combination with the smallness of the acetonitrile molecule allows for a reliable description especially of nonlinear optical properties. Additionally, it is possible with this approach to investigate the convergence behavior of the permanent local field with respect to the terms included in the multipolar expansion.

On the other hand, the approach can only be successful if the simulated liquid structure is accurate with respect to macroscopic electric properties. As in previous work, classical, nonpolarizable force fields will be employed in this work, using partial charges to describe the long-range Coulomb interactions. The performance of several force fields taken directly from the literature, or modified according to the results of the DLF analysis, will be analyzed in regard to their ability to predict the macroscopic linear and nonlinear electric properties of liquid acetonitrile.

The paper is organized as follows: the necessary theoretical framework is presented in section 2. The computed CH_3CN molecular NLO properties as well as the nonlinear macroscopic susceptibilities are presented in section 3. Finally, the main findings of our study are summarized in section 4.

* Corresponding author. E-mail: hreis@eie.gr.

10.1021/jp066630q CCC: $37.00
Published on Web 02/21/2007

2. Methods and Computational Details

a. Molecular Dynamics Simulations. We performed a series of molecular dynamics simulations of the neat liquid acetonitrile (CH_3CN). One goal of this study was the computation of the effect of the local field in quadrupolar and higher order approximation on the macroscopic susceptibilities of liquid CH_3CN. The potential which was employed for the classical, nonpolarized molecular dynamics simulation is given by the following expression:

$$\sum_{i<j}\left(\frac{A_{ij}}{R_{ij}^{12}}-\frac{B_{ij}}{R_{ij}^{6}}+\frac{q_iq_j}{R_{ij}}\right) \tag{1}$$

where A and B are the nonbonded Lennard-Jones (LJ) parameters and q are the partial atomic charges. In the present study, the initial q_i and LJ parameters were taken from Böhm et al.[10] After the computation of the local field with the inductive model described below, the partial charges were rescaled to conform to the average dipole moment of the molecule in this local field, yielding $q_N = -0.6509$ e, $q_{CN} = 0.6179$ e, $q_{CH} = -0.6908$ e, and $q_H = 0.2410$ e. The geometry of the molecule remained fixed during these simulations. Additional simulations were carried out with three other force fields, the flexible OPLS-AA potential developed by Jorgensen et al.,[11] a potential developed by Hloucha et al.,[12] based on an extensive ab initio study of the potential energy surface of acetonitrile dimers using symmetry adapted perturbation theory,[13] and the recently reported three site potential of Gee and van Gunsteren.[14]

In all simulations, the cubic unit box contained 256 molecules of CH_3CN, with the box size chosen to correspond to the experimental density, 0.776 g/cm^3,[15] of the pure liquid at 298 K and 1 atm, leading to an axis length of 28.232 Å. The simulation step was 2 fs, and the trajectories were recorded every 0.4 ps. Prior to recording, the system was equilibrated for 50 ps, using velocity scaling to speed up the equilibration process. Most of the molecular simulations were performed in the NVT canonical ensemble, using the Nosé−Hoover extended ensemble for the temperature control.[16] Additionally, some simulations were performed in the NPT ensemble, in order to check the performance of the employed potentials to model the density of liquid acetronitrile, using either the Melchionna modification of the Hoover barostat[17] or the Berendsen coupling.[18] The long-range electrostatic interactions between the atoms were computed by employing the Ewald summation approach,[19] using conducting boundary conditions. The molecular dynamics calculations were performed either with the DL_POLY molecular simulation package[20] or with the GROMACS package.[21] Some cross-checks were made to ensure that the results from the two simulation packages were comparable.

b. Induction Model. In the discrete local field approximation, as applied in this work, a molecule in a liquid environment is affected by local fields due to the charge distributions of the molecules of the surrounding environment. The molecular charge distribution of each molecule can be approximated by an nth-order electric multipole moment expansion about a point R,[22] with the corresponding multipole moments defined by

$$\mathbf{M}^{(n)} = \frac{1}{n!}\int_v (\underline{r}-\underline{R})^{[n]}\rho(\underline{r})\,\mathrm{d}v \tag{2}$$

where the superscript "[n]" denotes the n-fold tensor product, $\rho(\underline{r}) = \sum_s q_s\delta(\underline{r}-\underline{r}_s)$, is the charge density at position $\underline{r}$, $\mathbf{M}^{(n)}$ is the multipole moment, $\mathbf{M}^{(1)} = \mu$ corresponds to the dipole moment, $\mathbf{M}^{(2)} = Q$ is the quadrupole moment, $\mathbf{M}^{(3)} = O$ is the octupole moment, and $\mathbf{M}^{(4)} = H$ is the hexadecapole moment of the (overall neutral) molecule. All multipole moments refer to the center of nuclear charge. In quadrupolar approximation, the permanent local field $\underline{F}_k^{(0)}$ at site k, due to the surrounding molecules at sites k' and its corresponding gradient $\nabla\underline{F}_k^{(0)}$, with Cartesian components $F_{k\alpha\beta}^{(0)}$, can be expressed in the following way:

$$F_{k\alpha}^{(0)} = F_{k\alpha}^{(0),\mu} + F_{k\alpha}^{(0),Q} = \sum_{k'\neq k}^{N} T_{kk',\alpha\beta}^{(2)}\mu_{k'\beta}^{\mathrm{eff}} + \sum_{k'\neq k}^{N} T_{kk',\alpha\beta\gamma}^{(3)}Q_{k'\beta\gamma}^{\mathrm{eff}} \tag{3}$$

$$F_{k\alpha\beta}^{(0)} = F_{k\alpha\beta}^{(0),\mu} + F_{k\alpha\beta}^{(0),Q} = \sum_{k'\neq k}^{N} T_{kk',\alpha\beta\gamma}^{(3)}\mu_{k'\gamma}^{\mathrm{eff}} + \sum_{k'\neq k}^{N} T_{kk',\alpha\beta\gamma\delta}^{(4)}Q_{k'\gamma\delta}^{\mathrm{eff}} \tag{4}$$

where N is the number of molecules in the liquid. The Einstein summation convention is assumed for Cartesian indices α, β, ... , which appear twice in a product term. The $\mathbf{T}^{(n)}$ are multipole field tensors defined for relative positions $\underline{r}_{kk'} = \underline{r}_{k'} - \underline{r}_k$ as

$$\mathbf{T}_{kk'}^{(n)}(\underline{r}_{kk'}) = \nabla^{[n]}\frac{1}{|\underline{r}_{kk'}|} \tag{5}$$

The effective dipole and quadrupole moments of a molecule at site k' in the liquid are given in quadrupolar approximation by

$$\mu_{k'\alpha}^{\mathrm{eff}} = \mu_{k'\alpha}^{(0)} + \alpha_{k'\alpha\beta}^{0,(1,1)}(0;0)F_{k'\alpha}^{(0)} + \alpha_{k'\alpha\beta\gamma}^{0,(1,2)}(0;0)F_{k'\gamma\delta}^{(0)} \tag{6}$$

$$Q_{k'\alpha\beta}^{\mathrm{eff}} = Q_{k'\alpha\beta}^{(0)} + \alpha_{k'\alpha\beta\gamma}^{0,(2,1)}(0;0)F_{k'\alpha}^{(0)} + \alpha_{k'\alpha\beta\gamma\delta}^{0,(2,2)}(0;0)F_{k'\gamma\delta}^{(0)} \tag{7}$$

where $\alpha_{k'\alpha\beta}^{0,(1,1)}$, $\alpha_{k'\alpha\beta\gamma}^{0,(1,2)}$, $\alpha_{k'\alpha\beta\gamma}^{0,(1,2)}$, and $\alpha_{k'\alpha\beta\gamma\delta}^{0,(2,2)}$ are components of, respectively, the dipole−dipole second-order polarizability tensor, the dipole−quadrupole, the quadrupole−dipole third-order polarizability tensor, and the quadrupole−quadrupole fourth-order polarizability tensor. The tensors $\alpha_{k'\alpha\beta\gamma}^{0,(1,2)}$ and $\alpha_{k'\alpha\beta\gamma}^{0,(1,2)}$ are connected by the relationship $a_{i,jk}^{0,(1,2)} = a_{jk,i}^{0,(2,1)}$. The first superscript "0" on the polarizabilities expresses the fact that the corresponding properties are those of the *free* molecule; that is, hyperpolarizability contributions to the local fields are neglected. The superscript "(0)" on the multipole moments on the other hand denotes the permanent moments.

Specializing to the case of a replicated unit cell as obtained from the simulations and introducing the Lorentz-factor tensors $L^{(n)}$, computed in periodic boundary conditions with conducting boundaries, we can obtain from eqs 3, 4, 6, and 7 an implicit expression for the fields and field gradients which contains only known quantities:[23]

$$F_{k\alpha}^{(0)} = (\epsilon_0 V_{\mathrm{cell}})^{-1}\sum_{k'\neq k}^{N} L_{kk',\alpha\beta}^{(11)}[\mu_{k'\beta}^{(0)} + \alpha_{k',\beta\gamma}^{0,(1,1)}F_{k'\gamma}^{(0)} + \alpha_{k',\beta\gamma\delta}^{0,(1,2)}F_{k'\gamma\delta}^{(0)}] + (\epsilon_0 V_{\mathrm{cell}})^{-1}\sum_{k'\neq k}^{N} L_{kk',\alpha\beta\gamma}^{(12)}[Q_{k'\beta\gamma}^{(0)} + \alpha_{k',\beta\gamma\delta}^{0,(2,1)}F_{k'\delta}^{(0)} + \alpha_{k',\beta\gamma\delta\epsilon}^{0,(2,2)}F_{k'\delta\epsilon}^{(0)}] \tag{8}$$

$$F^{(0)}_{k\alpha\beta} = -(\epsilon_0 V_{\mathrm{cell}})^{-1} \sum_{k'\neq k}^{N} L^{(21)}_{kk',\alpha\beta\gamma}[\mu^{(0)}_{k'\gamma} + \alpha^{0,(1,1)}_{k',\gamma\delta} F^{(0)}_{k'\delta} + \alpha^{0,(1,2)}_{k',\gamma\delta\epsilon} F^{(0)}_{k'\delta\epsilon}] - (\epsilon_0 V_{\mathrm{cell}})^{-1} \sum_{k'\neq k}^{N} L^{(22)}_{kk',\alpha\beta\gamma\delta}[Q^{(0)}_{k'\gamma\delta} + \alpha^{0,(2,1)}_{k',\gamma\delta\epsilon} F^{(0)}_{k'\epsilon} + \alpha^{0,(2,2)}_{k',\gamma\delta\epsilon\iota} F^{(0)}_{k'\epsilon\iota}] \quad (9)$$

This expression can be solved for the local fields and field gradients by inversion or iteration.[23]

In addition to the pure quadrupole approximation, we also considered the effect of the *permanent* octopole $O^{(0)}$ and hexadecapole $H^{(0)}$ moments, in order to check the convergence of the fields and gradients with respect to order of the multipolar expansion. As the corresponding polarizabilities were not taken into account, the contributions of these multipoles, contracted with the corresponding Lorentz-factor tensor, simply add to the fields and gradients of eqs 8 and 9.

The dipole moment and dipole polarizability of the free molecule were taken from ref 7, while the quadrupole−dipole and quadrupole−quadrupole polarizabilities were computed numerically from finite field gradient differences of multipole moments computed at the MP2 level with the d-aug-cc-pVDZ basis set,[24] using a base field gradient value of 0.0001 au (Table 1). For these calculations, the Gaussian 98[25] suite of programs was employed. As in our previous work,[7] the experimental structural parameters determined by Costain were used for all of the quantum mechanical theoretical computations of the (hyper)polarizabilites.[26]

Solving the set of eqs 6−9 for each molecule in the simulation box and averaging over the molecules and the trajectories, the average local field and field gradient on a molecule immersed in the liquid is obtained. The electric properties of a molecule subject to these local fields are what we will call "effective" properties and will be denoted by the superscript "eff" in the following. Note that these correspond to the "solute" properties of ref 1. Using these properties, several experimentally determined macroscopic properties of the liquid acetonitrile have been computed: the dielectric constant ϵ_r, refractive indices $n(\omega)$, the electric field induced second-harmonic (EFISH) susceptibility $\chi^{(3)}_{ZZZZ}(-2\omega;\omega,\omega,0)$, where Z is the direction of the externally applied field in the laboratory system, and finally the third-harmonic generation (THG) signal $\chi^{(3)}_{ZZZZ}(-3\omega;\omega,\omega,\omega)$. The dielectric constant was evaluated by the following formula:[2,27]

$$\epsilon_r = \frac{\langle \underline{M}^2 \rangle - \langle \underline{M} \rangle^2}{3\epsilon_0 k_B T V} + n_\infty{}^2 \quad (10)$$

where ϵ_0 is the relative permittivity of the vacuum, k_B is the Boltzmann constant, and V is the volume of the simulated unit cell. The brackets denote averaging over the simulated ensemble and $\underline{M} = \Sigma_i \underline{\mu}^{\mathrm{eff}}$ is the instantaneous dipole moment, where μ^{eff} is given by eq 6. The nonorientational term $n_\infty{}^2$ is computed from the equation for the first susceptibility in the discrete local field theory approach; see, for example, eq 3 in ref 28. The term $\langle \underline{M} \rangle^2$, which is zero for an isotropic liquid, was found to be small ($\langle \underline{M}^2 \rangle > 500 \langle \underline{M} \rangle^2$, after averaging over ~1 ns) and was thus neglected.

TABLE 1: Static Electric Quadrupole (Q), Octupole (O), and Hexadecapole (H) Moments, Dipole−Quadrupole Polarizability $\alpha^{0,(1,2)}$, and Quadrupole−Quadrupole Polarizability $\alpha^{0,(2,2)}$ of Acetonitrile[a] (All Values Are in Atomic Units)

property	MP2
$Q^{(0)}_{ii}$	−6.665,−6.665,−7.998
$O^{(0)}_{iiz}, O^{(0)}_{yyy}$	−0.472,−0.472,−2.889,0.201
$H^{(0)}_{iiii}, H^{(0)}_{yyyz}$	−2.86,−2.86,−20.91,−0.16
$H^{(0)}_{iijj}, H^{(0)}_{xxyz}$	−0.95,−3.54,−3.54,0.16
$a^{0,(1,2)}_{x,ij}$	0.0,−2.169, −5.920, 0.0,0.0,−5.920
$a^{0,(1,2)}_{y,ij}$	−2.169,0.0,0.0,2.169,−5.920,0.0
$a^{0,(1,2)}_{z,ij}$	−1.8315,0.0,0.0,−1.8315,0.0,0.4812
$a^{0,(2,2)}_{xx,ij}$	29.2741,0.0,0.0,4.9448,3.6984,4.2060
$a^{0,(2,2)}_{yy,ij}$	4.9449,0.0,0.0,29.2741,−3.6984,4.206
$a^{0,(2,2)}_{zz,ij}$	4.206,0.0,0.0,4.206,0.0,145.065
$a^{0,(2,2)}_{xy,ij}$	0.0,12.1646,3.6984,0.0,0.0,0.0
$a^{0,(2,2)}_{xz,ij}$	0.0,3.698,55.2378,0.0,0.0,0.0
$a^{0,(2,2)}_{yz,ij}$	3.6984,0.0,0.0,−3.698,55.238,0.0

[a] The properties were computed at the experimental geometry[26] by employing the MP2 method with the d-aug-cc-pvDZ basis set. The double index ij runs over xx,xy,xz,yy,yz,zz.

The susceptibilities used here are defined by the following expansion of the macroscopic polarization:[29,30]

$$\frac{P(\omega_\sigma)}{\epsilon_0} = \sum_{\{\omega_\nu\}} K(-\omega_\sigma;\omega_1, \ldots, \omega_n)\chi^{(n)}(-\omega_\sigma;\omega_1, \ldots, \omega_n)E_{\omega_1}, \ldots, E_{\omega_n} \quad (11)$$

where n represents the number of input fields, $\chi^{(n)}$ is a (non)-linear optical susceptibility tensor of rank $n + 1$ and with units $(\mathrm{V\ m^{-1}})^{1-n}$ (in SI), K is a numerical factor depending on the specific NLO process, and $\omega_\sigma = \omega_1 + \ldots + \omega_n$. For the case of the EFISH process,[29] the value of $K(-2\omega;\omega,\omega,0)$ is equal to $^3/_2$; for THG, it is $K(-3\omega;\omega,\omega,\omega) = {}^1/_4$. Assuming that applied *optical* fields do not disturb the liquid structure, the THG susceptibility in discrete local field theory can be computed using the trajectories of the simulated unperturbed liquid, applying formulas for the calculation of the THG given previously; see, for example, ref 28. Due to the presence of a *static* electric field, a different approach is necessary for the EFISH susceptibility. To compute this property, an additional static electric field E_Z was applied during the molecular simulation, to perturb the orientational isotropy of the liquid. The average first $\chi^{(2)}_{ZZZ}(-2\omega;\omega,\omega;E_Z)$ and second $\chi^{(3\gamma)}_{ZZZZ}(-2\omega;\omega,\omega,0)$ nonlinear susceptibilities were then computed using the corresponding trajectories. If the field strength E_Z is chosen correctly, the final EFISH susceptibility $\chi^{(3)}_{ZZZZ}(-2\omega;\omega,\omega,0)$ is given by

$$\chi^{(3)}_{ZZZZ}(-2\omega;\omega,\omega,0) = \frac{\chi^{(2)}_{ZZZ}(-2\omega;\omega,\omega;E_Z)}{3E_Z} + \chi^{(3\gamma)}_{ZZZZ}(-2\omega;\omega,\omega,0) \quad (12)$$

where $\chi^{(2)}_{ZZZ}(-2\omega;\omega,\omega;E_Z)$ is given by[28]

$$\chi^{(2)}_{ZZZ}(-2\omega;\omega,\omega;E_Z) = (2\epsilon_0 V)^{-1} \sum_{k,IJK} d_{k,ZI}(2\omega)\beta^{\mathrm{eff}}_{k,IJK}(-2\omega;\omega,\omega)d_{k,ZJ}(\omega)d_{k,ZK}(\omega) \quad (13)$$

where the $d_{k,IJ}$ are elements of local field factor tensors[28] and the functional dependence on the external field on the right-

TABLE 2: Components of the Effective[a] and, in Parentheses, Free Molecule[b] Dipole Moment μ_z, Static Electronic Polarizability (α_{ii}), and First (β_{zii}) and Second (γ_{iijj}) Hyperpolarizability of Acetonitrile Computed at the HF, MP2, and CCSD Levels with the d-aug-cc-pVDZ Basis Set (All Values in Atomic Units)

	HF	MP2	CCSD
μ_z	2.194 (1.673)	2.067 (1.537)	
α_{xx}	24.01 (23.96)	24.63 (24.48)	24.66 (24.52)
α_{zz}	38.98 (38.42)	39.98 (38.88)	40.24 (39.13)
β_{zxx}	12.00 (−2.90)	21.01 (1.44)	20.88 (1.17)
β_{zzz}	72.84 (12.71)	130.12 (37.39)	132.32 (35.33)
			CC2
γ_{xxxx}	2518 (2323)	2950 (2690)	3307 (2975)
γ_{zzzz}	4992 (4244)	8066 (6327)	10090 (7834)
γ_{xxzz}	1225 (1043)	1657 (1345)	1906 (1340)
γ_{xxyy}	839 (774)	983 (897)	1102 (941)

[a] Local field value, $F_z = 0.0135$ au. [b] Taken from ref 7.

hand side of the equation manifests itself in the fact that the sum over the molecules does not vanish. To make a connection with the more familiar expression for the effective EFISH measurable obtained in the continuum approach, we note that the first term in eq 12 corresponds to the orientational term $f(2\omega)[f(\omega)]^2 f(0)(\beta_z^{\mathrm{eff}}(-2\omega;\omega,\omega)\mu_z^{(0)})/(5k_BT)$, as obtained by orientational averaging. Here, the f are Onsager−Lorentz local field factors, $\beta_z^{\mathrm{eff}} = {}^1/_3(\Sigma_i\,(\beta_{zii} + 2\beta_{izi}))$, where β_{ijk} is a component of the *effective* first hyperpolarizability, while $\mu_z^{(0)}$ is the dipole moment of the *free* molecule[1] and z is the direction of the molecular dipole moment in the molecular axis system. The second term in eq 12 corresponds to the nonorientational term $f(2\omega)[f(\omega)]^2 f(0)\gamma_{\mathrm{av}}^{\mathrm{eff}}(-2\omega;\omega,\omega,0)$.

All of the necessary effective frequency dependent molecular polarizabilities and first hyperpolarizabilities, needed for the computation of the susceptibilities, were computed at the CCSD level,[31] while second hyperpolarizabilities, which are generally less important for the EFISH signal of strongly polar molecules, were computed at the computationally cheaper CC2 level of theory,[32] by employing the DALTON software.[33] As in our previous work, the frequency dispersion of γ computed at the CC2 level was employed as a scaling factor for the static MP2/d-aug-cc-pVDZ properties, as the static CC2 values were not considered accurate. All of the studied molecular NLO properties are reported in atomic units, while the susceptibilities are given in Systeme International (SI) units. Conversion factors to other units are given in ref 34.

3. Results and Discussion

a. Effective Molecular Properties of CH_3CN in the Liquid. The molecular properties of the free molecule, that is, dipole moment, quadrupolar moment, and dipole−quadrupole and quadrupole−quadrupole polarizabilities, used in the computation of the local field according to eqs 8 and 9, are presented in Tables 1 and 2.

As mentioned in the previous section, the MD simulations were started using the original force field developed by Böhm et al.[10] The analysis of the resulting trajectories according to the hexadecapolar induction model yielded an average effective dipole moment of 1.96 au, significantly larger than the dipole moment of the molecule at the reference geometry obtained using the partial charges of force field of Böhm et al. 1.61 au. Additionally, the relative permittivity obtained was considerably lower than the experimental value (see section 3b) and Table 5). Thus, the partial charges used in the simulation were rescaled to yield the dipole from the induction model for the reference geometry, and the simulation was repeated using the modified force field. With the new trajectories, the relative permittivity was in good agreement with the experimental value. Thus, the data from this simulation were used for a complete analysis.

The average local field on a CH_3CN molecule obtained in hexadecapolar approximation was $F_z^{(0)} = 0.0135$ au (6.9 GV/m), parallel to the molecular dipole moment; perpendicular components were at least 1 order of magnitude smaller and neglected. Similarly, the local field gradients were small (largest absolute value 0.0013 au). Test calculations showed that the field gradients had nearly no influence on the electric properties and were thus neglected, too.

In order to analyze the contribution of the different multipolar orders to the permanent local field, we repeated the induction analysis, including only the dipolar terms in eq 8 and obtained a field of $F_z^{(0)} = 0.012$ au, showing clearly the dominance of

TABLE 3: Components of the Effective[a] and, in Parentheses, Free Molecule[b] Frequency[c] Dependent Polarizabilities, First- and Second-Order Hyperpolarizability Components of Acetonitrile Computed at the CC2 and CCSD Level with the d-aug-cc-pVDZ Basis Set (All Values Are in Atomic Units)

CCSD		CC2		
			$\gamma(-2\omega;\omega,\omega,0)$	$\gamma(-3\omega;\omega,\omega,\omega)$
$\alpha_{xx}(\omega)$	24.81 (24.66)	γ_{xxxx}	3647 (3240)	3512
$\alpha_{zz}(\omega)$	40.57 (41.59)	γ_{zzzz}	11469 (8624)	10912
$\alpha_{xx}(2\omega)$	25.25	γ_{xxzz}	2128 (1634)	2040
$\alpha_{zz}(2\omega)$	41.58	γ_{zxzx}	2168 (1658)	
$\beta_{xxz}(-2\omega;\omega,\omega)$	23.00 (1.37)	γ_{xzzx}	2166 (1648)	
$\beta_{zxx}(-2\omega;\omega,\omega)$	23.77 (1.76)	γ_{xxyy}	1208 (1076)	1170
$\beta_{zzz}(-2\omega;\omega,\omega)$	144.95 (37.79)			

[a] $F_z = 0.0135$ au. [b] Values taken from ref 7. [c] Values at $\omega = 0.0428$ au, except for $\gamma(-3\omega;\omega,\omega,\omega)$, where $\omega = 0.0239$ αu.

TABLE 4: Nonlinear Macroscopic EFSHG Susceptibilities of Liquid CH_3CN, Computed at Various Macroscopic Applied Fields[a]

	applied fields: E_z ($\times 10^7$ V/m)			
susceptibilities	2.0	3.0	5.0	14.0
$\chi_{zzz}^{(2)}(-2\omega;\omega,\omega;E_z)/10^{-12}$ m V^{-1}	0.152	0.236	0.336	0.979
$\chi^{(3)\gamma}(-2\omega;\omega,\omega,0)/10^{-24}$ m^2 V^{-2}	208.74	207.93	209.56	216.12
$\chi^{(3)}(-2\omega;\omega,\omega,0)/10^{-21}$ m^2 V^{-2} [b,c]	2.74	2.83	2.45	2.54
experimental values				
$\chi^{(3)}(-2\omega;\omega,\omega,0)/10^{-21}$ m^2 V^{-2}	1.77[b]			

[a] The values were computed using frequency dependent molecular properties at $\omega = 0.0428$ au, obtained with the local field value $F_z = -6.954 \times 10^9$ V/m (∼0.0135 au). [b] $\omega = 0.0428$ au. [c] $\chi^{(3)}(-2\omega;\omega,\omega,0) = \chi^{(3)\gamma}(-2\omega;\omega,\omega,0) + [\chi^{(2)}(-2\omega;\omega,\omega;E)/3E]$.

TABLE 5: Simulated Density ρ, Relative Permittivity ϵ, and Orientational Contribution to the EFISH Signal $\chi^{(2)} \equiv \chi^{(2)}(-2\omega;\omega,\omega;0)$ at 298 K, Obtained with Different Force Fields

force field	ρ/(g cm^{-3})	ϵ	$\chi^{(2)}/(10^{-21}$ m V$^{-1})$
Böhm, usc[b]	0.859	31.8	2.02
Böhm, sc[c]	0.924	35.3	2.29 (2.50)[a]
OPLS-AA, usc[b]	0.748	29.4	1.76
OPLS-AA, sc[c]	1.038	30.6	2.04
ANC1	0.836	33.7	2.15
ANL	0.882		
exptl	0.776	35.84	1.76[a]

[a] Including the nonorientational $\chi^{(3)\gamma}(-2\omega;\omega,\omega,0)$ term. [b] With original partial charges. [c] With partial charges scaled to conform to the induced dipole moment from the DLF analysis.

the dipole−dipole interactions, as the higher order multipoles contribute only about 11% to the total value. Interestingly, the contributions of the permanent octopole $O^{(0)}$ and hexadecapole $H^{(0)}$ moments to $F_z^{(0)}$ are relatively large and with an opposite sign than the dipole and quadrupole contributions. In *quadrupolar* approximation only, that is, without the $O^{(0)}$ and $H^{(0)}$ contributions, the field is $F_z^{(0)} = 0.015$ au, that is, about 25% larger than in the dipolar approximation.

Adding an electric field of $E_z = 0.0135$ au to the Hamiltonian, the *effective* static and frequency dependent electric properties listed in Tables 2 and 3 were computed, denoted by p^{eff}, with $p = \mu$, α, β, and γ. For comparison, the properties of the free molecule (p^{gas}) are also listed. They were taken from the first part of this study, ref 7. They had been found to be in good agreement with available experimental and high-quality theoretical results.

As found in our previous study, the MP2 level captures most of the correlation effects obtained at the CCSD level. In ref 7, it was also found that CC2 overshoots the correlation effects considerably. Thus, the CC2 values were only used to scale the static MP2 values with the frequency dispersion. Generally, electronic correlation is clearly important for the electric properties of CH_3CN and cannot be neglected.

The permanent local field obtained here is nearly twice the value 0.0071 au, which we had obtained using the Onsager reaction field model in part I of this study,[7] where we also found generally a good agreement of several linear and nonlinear susceptibilities in the framework of the Onsager model with experimental values.

The value of μ is equal to 2.067 au at the MP2 level. This value is substantially larger than the only available experimental estimate of this property in the liquid of 1.77 ± 0.04 au, which was obtained from integrated far-infrared spectra using several simplifying approximations.[35] The value obtained using the Onsager model is 1.8 au.[7] In this context, we may note the report of an investigation of the induced electronic polarization in liquid acetonitrile using a sequential Monte Carlo/quantum mechanics method.[36] Using the unchanged potential of Böhm et al., this model yields an effective dipole moment of 1.847 ± 0.08 au, computed at the MP2/aug-cc-pVTZ level, in good agreement with the experimental estimate and considerably smaller than our value, although similar potentials were employed. Closer inspection of the method used in ref 36 shows, however, that the local field computed in the model does not include the reaction field contribution, only the contribution stemming from the unpolarizable partial charges. Clearly, the field and thus also the average effective dipole moment will be considerably smaller without this essential contribution. This holds also for the value reported by Ohba and Ikawa,[37] who used the original force field of Böhm et al. in a molecular dynamics simulation, and computed then the total induced dipole using the molecular polarizability and the permanent local field arising from the nonpolarizable partial charges of the environment. In fact, we can compute a comparable quantity by neglecting all polarizabilities in eqs 8 and 9, thus calculating the local field due only to the gas-phase multipole moments. In this way, one obtains a permanent local field value of $F_z = 0.0093$ au, which leads to $\mu_z = 1.89$ au, in good agreement with refs 36 and 37.

In another study, Jensen et al. report an increase of 25% for the dipole moment of an acetonitrile molecule in going from the gas to the liquid[38] using the discrete reaction field model, which is more similar to our method. In this QM/MM model, the response of a solute molecule is computed quantum mechanically by density functional theory (DFT) directly during the simulation. The surrounding solvent molecules are approximated by *polarizable* point charges, thus taking into account both direct and reaction field contributions. The fact that this method also uses the polarizable charges in the molecular simulation could be a hint that our use of nonpolarizable charges in the molecular dynamics leads to an overestimation of the permanent local field. Unfortunately, the other parameters of the simulation potential are not specified in ref 38; thus, a more direct comparison with our values is not possible. A similar increase of the dipole moment from gas to liquid to that reported by Jensen et al. was obtained by Vande Vondele et al. using ab initio molecular dynamics simulations, employing DFT with the BLYP functional.[39]

An interesting comparison is possible, however, with the work of Richardi et al.[40] They performed molecular dynamics simulations as well as computations in the framework of a generalized self-consistent mean field approach combined with the molecular Ornstein−Zernike theory in the hypernetted chain approximation (MOZ/GSCMF). The electrostatic part of the potential was described by partial charges computed for an optimized isolated molecule, and thus slightly smaller than the original charges of the potential of Böhm et al., and either one-site dipole−dipole or distributed (m,n) polarizabilities, with $(m,n) = 0,1$, corresponding to charge and dipole terms. The distributed polarizabilities were computed using a topological partitioning of the wave function[41] developed by Bader (Atoms in Molecules approach),[42] for the isolated molecule. The remaining van der Waals interactions were described by the parameters used in the potential of Böhm et al. With this potential, an increase in the molecular dipole moment of ∼31% for the one-site polarizability description and ∼24% for the distributed polarizability model was obtained. In related work, Fries et al.[43] applied the self-consistent mean field/hypernetted chain approach using again the Lennard-Jones parameters from Böhm et al. and one-site dipole and quadrupole moments as well as dipole−dipole polarizabilities for liquid acetonitrile. They report an increase of 36% for the dipole moment, very similar to our findings. Similar enhancements were found by Richardi et al.[44] with a similar method, but including also octopole and hexadecapole moments.

Thus, from previous work of Richardi et al.[40,44] and Fries et al.,[43] we conclude that the inclusion of polarizabilities in the simulation potential of Böhm et al. does probably not yield a smaller effective dipole moment in the liquid as obtained by us. Only if *distributed* polarizabilities are employed, one may expect a small decrease.

In Table 2, the static effective and gas-phase (hyper)-polarizabilities are presented, while frequency dependent results for α, β, and γ for electric field induced second-harmonic (EFISH) generation at $\omega = 0.0428$ au ($\lambda = 1064$ nm) and γ for third-harmonic generation (THG) at $\omega = 0.0239$ au ($\lambda = 1932$ nm) are listed in Table 3. Comparison of effective and isolated properties shows a similar pattern to that observed previously with other systems: the permanent local field has a small effect on the linear polarizability, a medium large effect on dipole moments and second hyperpolarizabilities, and a strong effect on first hyperpolarizabilities. The latter effects are even more pronounced for acetonitrile, due to the small absolute values of the components of β.

b. Macroscopic Nonlinear Optical Properties. The following macroscopic susceptibilities were computed in the DLF approach for liquid acetonitrile: dielectric constant ϵ_r, refractive indices $n(\omega)$, EFISH susceptibility $\chi^{(3)}(-2\omega;\omega,\omega,0)$, and third-

harmonic generation (THG) susceptibility $\chi^{(3)}(-3\omega;\omega,\omega,\omega)$. For all of these quantities, experimental data are available and allow a direct comparison with the computed values. The computation of the dielectric constant by the model used in the present work (eq 10) accounts for orientational effects caused by the effective dipole moment as well as for the nonorientational induced effects. The contribution of the higher than dipolar terms to $\langle \underline{M}^2 \rangle$ is not unimportant; including them, the orientational contribution to ϵ_r is 33.5, while only including the dipolar terms yields a value of 30.5. Adding the nonorientational term ϵ_∞, which is equal to 1.79, the final estimate for the dielectric constant in hexadecapolar approximation is $\epsilon = 35.3$. This is in good agreement with the experimental value 35.8445. The predicted refractive index $n(\omega)$ at $\omega = 0.0856$ ($\lambda = 532$ nm) is 1.348, in very good agreement with the experimental value $n(\omega) = 1.348$.[46] We note that similar values for ϵ as found here were obtained by Richardi et al.[40] with the GSCMF/MOZ approach (34.8 with the one-site dipole−dipole polarizability, 35.8 with distributed charge and dipole polarizabilities), by Fries et al.[43] with the SCMF/HNC approach, who obtained 35.2 with the dipole + quadrupole + anisotropic dipole−dipole polarizability description, and by Richardi et al.,[44] who report 36.4−37.3 using multipoles up to hexadecapole and dipole−dipole polarizabilities.

As our model for liquid acetonitrile appears to describe the linear susceptibilities very well, we proceeded to compute the nonlinear EFISH $\chi^{(3)}_{zzzz}(-2\omega;\omega,\omega,0)$ and THG $\chi^{(3)}_{iiii}(-3\omega;\omega,\omega,\omega)$ susceptibilities, according to the methods outlined in section 2b. For $\chi^{(3)}_{iiii}(-3\omega;\omega,\omega,\omega)$ at $\omega = 0.0239$ au ($\lambda = 1907$ nm), a value of 1.89 10^{-22} $(m/V)^2$ was obtained by averaging over the three diagonal components. This value includes the cascading effect, but as found previously for other liquids,[23,47] the cascading contribution is quite small, only 0.07 $\times$ 10^{-22} $(m/V)^2$ (4%). The corresponding experimental THG value, after recalibration to the latest calibration value[48] and conversion to the conventions used here, is 1.48 $\times$ 10^{-22} $(m/V)^2$,[7,38,49] considerably smaller than our computed value. A similar value (1.79 $\times$ 10^{-22} $(m/V)^2$) to that found here was reported by Jensen et al. using the polarizable DRF model.[38]

To compute the EFISH susceptibility according to the procedure outlined in section 2b), it is necessary to run separate molecular simulations in an external electric field. The optimum field strength is not known a priori; if it is too low, the signal/noise ratio may be too low to extract a reliable value; if it is too high, one may probe unwanted additional effects nonlinear in the *static* field. Thus, four simulations with different field values were conducted, with external fields E_Z in the range (2−14) $\times$ 10^7 V/m; see Table 4. We note that static fields applied in experimental EFISH measurements are somewhat lower; for example, in ref 40, an applied field strength of $\sim 5 \times 10^6$ V/m is reported. The values for $\chi^{(2)}_{zzz}(-2\omega;\omega,\omega;E_Z)$ at $\omega = 0.0428$ au ($\lambda = 1064$ nm) obtained after DLF analysis are in a very good linear relationship to the applied field E_Z; see Figure 1. In Figure 2, we show the running averages of $\chi^{(2)}_{zzz}(-2\omega;\omega,\omega;E_Z)$, for $E_Z = 2 \times 10^7$ V/m and 5×10^7 V/m, as the relative difference from the final value, to demonstrate the convergence behavior of this quantity; for comparison, the running average of the relative difference from the final value of $\langle \underline{M}^2 \rangle$, which is also known to be slowly convergent,[51] is shown, too. It is seen that the nonlinear susceptibilities are much slower convergent than $\langle \underline{M}^2 \rangle$. Linear regression of $\chi^{(2)}_{zzz}(-2\omega;\omega,\omega;E_Z)$ against E_Z yields $\chi^{(2)}_{zzz}(-2\omega;\omega,\omega;0) = 2.29 \times 10^{-21}$ $(m/V)^2$. Adding the averaged nonorientational term yields finally $\chi^{(2)}_{zzz}(-2\omega;\omega,\omega;0) = 2.50$ 10^{-21} $(m/V)^2$, again considerably larger than the experimental value, 1.76 $\times$ 10^{-21} $(m/V)^2$, corrected for the latest reference and the conventions applied here.[7,37,52,53]

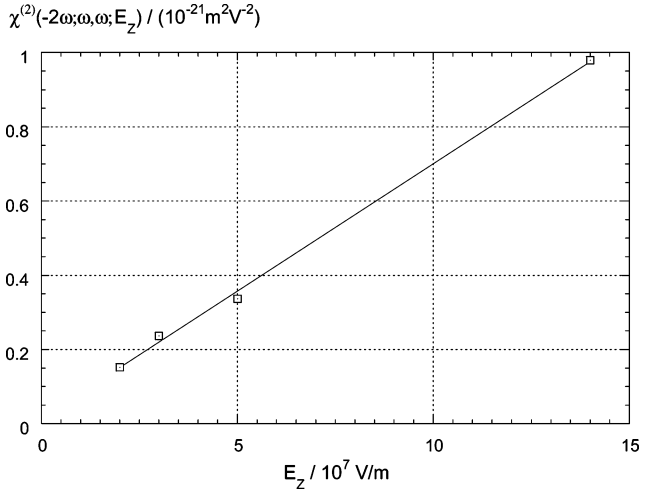

Figure 1. . Plot of $\chi^{(2)}(-2\omega;\omega,\omega;E)$ versus E.

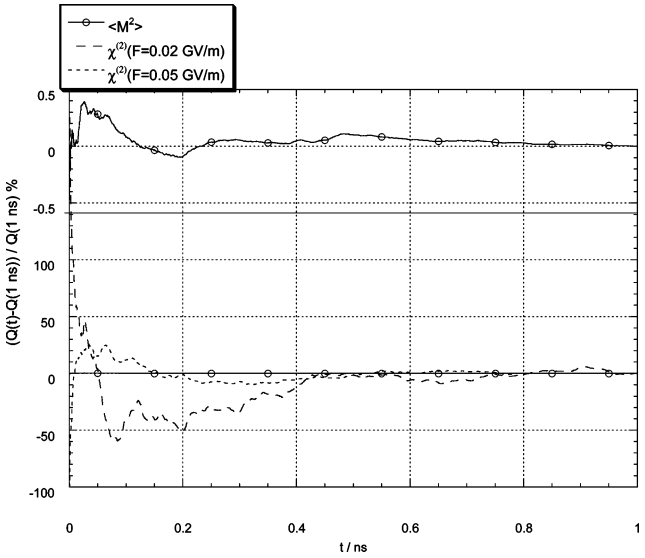

Figure 2. . Running averages of $[Q(t) - Q(1\text{ ns})]/Q(1\text{ ns})$ (in %) of $Q = \chi^{(2)}(-2\omega;\omega,\omega;E)$ for $E = 2 \times 10^7$ V/m and 5×10^7 V/m as well as $Q = \langle M^2 \rangle$; the upper part shows $Q = \langle M^2 \rangle$ with an enlarged scale.

Thus. it seems that the simulation model applied is not able to reproduce the experimental nonlinear susceptibilities very well. To investigate this apparent failure of the MD + DLF combination a bit further, we conducted additional computations. The large difference of the dipole moment as described by the original force field of Böhm et al. and the value obtained from polarized induction models points to a possible difficulty in the partitioning of the intermolecular interactions on short-range and Coulomb terms within this force field. Thus, it seemed worthwhile to test other force fields reported in the literature with respect to their performance for the prediction of dielectric properties. The work of Richardi et al.,[40,44] Fries et al.,[43] and Jensen et al.[38] indicates that the use of polarizabilities and/or higher multipole moments in the force fields does not lead to significantly better dielectric properties compared to standard force fields employing nonpolarizable partial charges. Therefore, we focused our attention on nonpolarizable standard force fields, which differ in the Lennard-Jones parameters and/or partial charges.

We furthermore concentrated on the prediction for three properties of liquid acetonitrile which should be described

reasonably well by any force field aiming at accurate dielectric properties: the liquid density ρ, obtained from NPT simulations, the dielectric constant ϵ, and the orientational term of the EFISH signal $\chi^{(2)}(-2\omega;\omega,\omega;E_Z)$ as computed from NVT simulations, using the experimental density. For the latter property, which requires the *effective* molecular electric properties according to eq 13, the electric properties as computed in the permanent local field of the scaled force field of Böhm et al. given in Table 3 were employed to keep the number of necessary computations at a manageable level. In most cases, the absolute value of permanent local field obtained was lower than for the scaled force field of Böhm et al. Thus, the neglect of the nonorientational $\chi^{(3)\gamma}$ term compensates partially for this approximation, when the predicted values are compared with experiment.

Five additional force fields were employed in the molecular dynamics simulation step: the original force field of Böhm et al. with unscaled partial charges, the three-site force field recently developed by Gee and van Gunsteren,[14] the potential developed called ANC1 by Hloucha et al.,[12] based on an extensive ab initio study of the potential energy surface of acetonitrile dimers using symmetry adapted perturbation theory,[13] and the OPLS-AA potential developed by Jorgensen et al.,[11] which includes intramolecular flexibilities. The latter was employed first with the original partial charges, and then with the partial charges scaled to yield the total dipole moment obtained from the induction analysis.

As Table 5 shows, all force fields, except the unscaled OPLS-AA force field, overestimate the densities. This also happened unfortunately for the three-site ANL force field, which otherwise appeared to be a very promising force field, as it has been reported to reproduce several properties of the liquid well, including the density and the relative permittivity, computed in approximation of nonpolarizable partial charges.[14] However, the density we obtained was nearly 14% larger than the experimental value, overall the worst performance for all of the unscaled force fields. Therefore, we did not pursue this force field further. The discrepancy may be due to the larger temperature used by us (298 K versus 293 K), or due to other differences in the two simulations.

For the other force fields, one finds that ϵ_r is generally lower and $\chi^{(2)}$ is generally larger than the experimental value, with a nearly linear relationship between the two quantities; both are also positively correlated with the simulated density. Comparison of the densities obtained for two scaled and unscaled force fields shows that the Coulomb interactions have a large influence on the average structure of the bulk liquid, as has also been observed by Ohba and Ikawa.[37] In addition, these authors showed that the average *local* structure as determined by X-ray and neutron scattering experiments is very little affected by Coulomb interactions. This means that Coulomb interactions are probably of minor importance at short range but essential at long range in acetonitrile. Usually, the emphasis in force field development is on accurate short-range parameters. Partial charges employed in force fields are generally determined by fitting to the electric potential computed beyond the van der Waals surface or by fitting to the potential surface of the acetonitrile dimer. Both methods do not take into account cooperative and long-range effects, which apparently are important in liquid acetonitrile. The partial charges thus determined may therefore lead to inadequate force fields as far as dielectric properties and other quantities strongly dependent on electrostatic interactions are concerned. For reliable predictions of these properties, a different method for the determination of force field parameters may be necessary, which puts more emphasis on the cooperative and long-range nature of the Coulomb interactions, and maybe less on the short-range parameters.

4. Summary and Conclusions

In this work, the microscopic and macroscopic linear and nonlinear optical and dielectric properties of liquid acetonitrile have been computed in a combined molecular dynamics/discrete local field approach using different classical, nonpolarizable force fields. The permanent local field was approximated by a multipolar expansion in which up to hexadecapolar terms have been included. With this simple model, we can interpret the origin and the significance of the environmental electrostatic interactions on the macroscopic NLO properties. It was found that the permanent local field is dominated by the dipole−dipole interactions, although the contribution of the higher multipoles may not be negligible for accurate predictions.

The linear and nonlinear dielectric properties obtained were found to depend considerably on the force field employed in the molecular dynamics step. In order to obtain a reasonable dielectric constant, the partial charges of literature force fields have to be increased. However, the rescaled force fields do not predict the liquid density and the nonlinear optical properties correctly. This is in contrast to the simple continuum approach in the form of the Onsager−Lorentz model applied in the first part of the series,[7] which was able to predict both linear and nonlinear properties of the liquid in good agreement with experiment. Comparison with previous work, which replaced the nonpolarizable partial charges in the force field of Böhm et al. by polarizable charges or higher order multipoles in the molecular dynamics step, indicates that these more accurate force fields do not lead to better dielectric properties than nonpolarizable force fields employing partial charges to describe Coulomb interactions. The same conclusion can be drawn by comparison with the work of Jensen et al.,[38] who employ a polarizable force field and obtain good linear optical properties but a too large nonlinear optical susceptibility in comparison with experiment, similarly to what we found when employing nonpolarizable force fields in the simulation step. The tentative conclusion drawn from this work is that the accurate description of linear and nonlinear dielectric properties of polar liquids as acetonitrile in discrete local field models requires a different approach to the development of the terms describing Coulomb interactions in force fields employed in the molecular simulation step.

References and Notes

(1) Wortmann, R.; Bishop, D. M. *J. Chem. Phys.* **1998**, *108*, 1001.
(2) Böttcher, C. *Theory of Electric Polarization*; Elsevier: Amsterdam, The Netherlands, 1973.
(3) (a) Cammi, R.; Cossi, M.; Menucci, B.; Tomasi, J. *J. Chem. Phys.* **1996**, *105*, 10556. (b) Munn, R.; Luo, Y.; Macak, P.; Ågren, H. *J. Chem. Phys* **1998**, *98*, 7159. (c) Luo, Y.; Macak, P.; Mikkelsen, K. V. *Chem. Phys. Lett.* **1997**, *275*, 145.
(4) Prasad, P. N.; Williams, D. J. Introduction to Nonlinear Optical Effects. *Molecules and Polymers*; Wiley: New York, 1991.
(5) Stähelin, M.; Burland, D. M.; Rice, J. E. *Chem. Phys. Lett.* **1992**, *192*, 245.
(6) (a) Levine, B.; Bethea, C. *J. Chem. Phys.* **1976**, *65*, 2429. (b) Teng, C.; Garito, A. *Phys. Rev. Lett.* **1983**, *50*, 350.
(7) Reis, H.; Papadopoulos M. G.; Avramopoulos, A. *J. Phys. Chem. A* **2003**, *107*, 3907.
(8) Evans, G. J. *Adv. Chem. Phys.* **1985**, *63*, 293, 377.
(9) Kaatz, P.; Shelton, D. P. *Phys. Rev. Lett.* **2000**, *82*, 1224. Shelton, D. P. *Chem. Phys. Lett.* **2000**, *325*, 513.
(10) Böhm, H. J.; McDonald, I. R.; Madden, P. A. *Mol. Phys.* **1983**, *49*, 347.
(11) Price, M. L. P.; Ostrovsky, D.; Jorgensen, W. L. *J. Comput. Chem.* **2001**, *22*, 1340.

(12) Hloucha, M.; Sum, A. K.; Sandler, S. I. *J. Chem. Phys.* **2000**, *113*, 5401.
(13) Bukowski, R.; Szalewicz, K.; Chabalowski, C. F. *J. Phys. Chem. A* **1999**, *103*, 7322.
(14) Gee, P. J.; Gunsteren, W. F. *Mol. Phys.* **2006**, *104*, 477.
(15) Riddick, J. A.; Bunger, W. B.; Sakano, T. K. *Techniques of Chemistry, Organic Solvents, Physical Properties and Methods of Purification*, 4th ed.; Wiley: New York, 1986.
(16) Hoover, W. G. *Phys. Rev. A* **1985**, *31*, 119; **1986**, *34*, 2499. Nose, S. *Mol. Phys.* **1986**, *57*, 187.
(17) Melchionna, S.; Cicotti, G.; Holian, B. L. *Mol. Phys.*, **1993**, *78*, 533.
(18) Berendsen, H. J. C.; Postma, J. P. M.; DiNola, A.; Haak, J. R. *J. Chem. Phys.* **1984**, *81*, 3684.
(19) Allen M. P.; Tildesley, D. J. *Computer Simulation of Liquids*; Clarendon Press: Oxford, U.K., 1987.
(20) Smith, W.; Leslie, M.; Forrester, T. R. *DL_POLY 2.14*; CCLRC, Daresbury Laboratory: Daresbury, Warrington, U.K., 2003.
(21) Berendsen, H. J. C.; van der Spoel, D.; van Drunen, R. *Comput. Phys. Commun.* **1995**, *91*, 43. Lindahl, E.; Hess, B.; van der Spoel, D. *J. Mol. Model.* **2001**, *7*, 306.
(22) Applequist, J. *J. Math. Phys.* **1983**, *24*, 736.
(23) Reis, H.; Papadopoulos, M. G.; Grzybowski, A. *J. Phys. Chem. B* **2006**, *110*, 18537.
(24) Dunning, T. H., Jr. *J. Chem. Phys.* **1989**, *90*, 1007.
(25) Frisch, M. J.; Trucks, G. W.; Schlegel, H. B.; Scuseria, G. E.; Robb, M. A.; Cheeseman, J. R.; Zakrzewski, V. G.; Montgomery, J. A., Jr.; Stratmann, R. E.; Burant, J. C.; Dapprich, S.; Millam, J. M.; Daniels, A. D.; Kudin, K. N.; Strain, M. C.; Farkas, O.; Tomasi, J.; Barone, V.; Cossi, M.; Cammi, R.; Mennucci, B.; Pomelli, C.; Adamo, C.; Clifford, S.; Ochterski, J.; Petersson, G. A.; Ayala, P. Y.; Cui, Q.; Morokuma, K.; Malick, D. K.; Rabuck, A. D.; Raghavachari, K.; Foresman, J. B.; Cioslowski, J.; Ortiz, J. V.; Baboul, A. G.; Stefanov, B. B.; Liu, G.; Liashenko, A.; Piskorz, P.; Komaromi, I.; Gomperts, R.; Martin, R. L. Fox, D. J.; Keith, T.; Al-Laham, M. A.; Peng, C. Y.; Nanayakkara, A.; Gonzalez, C.; Challacombe, M.; Gill, P. M. W.; Johnson, B.; Chen, W.; Wong, M. W.; Andres, J. L.; Gonzalez, C.; Head-Gordon, M.; Replogle, E. S.; Pople, J. A. *Gaussian 98*, revision A.9; Gaussian, Inc.: Pittsburgh, PA, 1998.
(26) Costain, C. C. *J. Chem. Phys.* **1958**, *22*, 864.
(27) Caillol, J. M.; Levesque, D.; Weis, J. J.; Kusalik, R. G.; Patey, G. N. *Mol. Phys.* **1985**, *55*, 65.
(28) Reis, H.; Papadopoulos, M. G.; Munn, R. W. *J. Chem. Phys.* **1998**, *109*, 6828.
(29) Butcher, P. N. *Nonlinear Optical Phenomena* Bulletin 200, Eng., Expt., Station, Ohio State University, 1965.
(30) Hanna, D. C.; Yuratich, M. A.; Cotter, D. *Nonlinear Optics of Free Atoms and Molecules*; Springer: Berlin, Heidelberg, 1979.
(31) Purvuis, G. D., III; Bartlett, R. J. *J. Chem. Phys.* **1982**, *76*, 1910.
(32) Christiansen, O.; Koch, H.; Jørgensen, P. *Chem. Phys. Lett.* **1995**, *243*, 409.
(33) Helgaker, T.; Jensen, H. J. Aa.; Joergensen, P.; Olsen, J.; Ruud, K.; Aagren, H.; Auer, A. A.; Bak, K. L.; Bakken, V.; Christiansen, O.; Coriani, S.; Dahle, P.; Dalskov, E. K.; Enevoldsen, T.; Fernandez, B.; Haettig, C.; Hald, K.; Halkier, A.; Heiberg, H.; Hettema, H.; Jonsson, D.; Kirpekar, Klopper, W.; S.; Kobayashi, R.; Koch, H.; Mikkelsen, K. V.; Norman, P.; Packer, M. J.; Pedersen, T. B.; Ruden, Salek, P.; T. A.; Sanchez, A.; Saue, T.; Sauer, S. P. A.; Schimmelpfennig, B.; Sylvester-Hvid, K. O.; Taylor, P. R.; Vahtras, O. *DALTON*, release 2.0; 2004.
(34) μ, 1 au = 8.4783×10^{-31} C m; Q, 1 au = $4.486\,55 \times 10^{-40}$ C m^2; $\alpha^{(1,1)}$, 1 a.u = $0.148\,174 \times 10^{-24}$ esu = 0.1649×10^{-40} (C^2 m^2)/J; $\alpha^{(1,2)}$, 1 au = $0.087\,25 \times 10^{-50}$ (C^2 m^3)/J = 0.0784×10^{-32} esu; $\alpha^{(2,2)}$, 1 au = $0.046\,17 \times 10^{-60}$ (C^2 m^4)/J = $0.041\,496 \times 10^{-40}$ esu; β, 1 au = $0.863\,993 \times 10^{-32}$ esu = $0.320\,662 \times 10^{-52}$ (C^3 m^3)/J^2; γ, 1 au = $0.503\,717 \times 10^{-39}$ esu = $0.623\,597 \times 10^{-64}$ (C^4 m^4)/J^3; $\chi^{(2)}$ (m V^{-1}) = 4.189×10^{-4} $\chi^{(2)}$ (esu); $\chi^{(3)}$ (m^2 V^{-2}) = 1.40×10^{-8} $\chi^{(3)}$ (esu).
(35) Ohba, T.; Ikawa, S. *Mol. Phys.* **1991**, *73*, 985.
(36) Rivelino, R.; Cabral, B. J. C.; Coutinho, K.; Canuto, S. *Chem. Phys. Lett.* **2005**, *407*, 13.
(37) Ohba, T.; Ikawa, S. *Mol. Phys.* **1991**, *73*, 999.
(38) Jensen, L.; Swart, M.; v. Duijnen, P. Th. *J. Chem. Phys.* **2005**, *122*, 34103.
(39) Vande Vondele, J.; Lynden-Bell, R.; Meijer, E. J.; Sprik, M. *J. Phys. Chem. B* **2006**, *110*, 3614.
(40) Richardi, J.; Fries, P. H.; Soetens, J.-C. *J. Mol. Liq.* **2000**, *88*, 209.
(41) Ángyán, J. G.; Jansen, G.; Loos, M.; Hättig, C.; Hess, B. A. *Chem. Phys. Lett.* **1994**, *219*, 267.
(42) Bader, R. F. W. *Atoms in Molecules—A Quantum Theory*; Clarendon: Oxford, U.K., 1994.
(43) Fries, P. H.; Richardi, J.; Krienke, H. *Mol. Phys.* **1997**, *90*, 841.
(44) Richardi, J.; Fries, P. H.; Krienke, H. *Mol. Phys.* **1999**, *96*, 1411.
(45) Barthel, J.; Kleebauer, M.; Buchner, R. *J. Solution Chem.* **1995**, *24*, 1.
(46) Norman, P.; Luo, Y.; Ågren, H. *J. Chem. Phys.* **1997**, *107*, 9535.
(47) Reis, H.; Papadopoulos, M. G.; Theodorou, D. N. *J. Chem. Phys.* **2001**, *114*, 876.
(48) Bosshard, C.; Gubler, U.; Kaatz, P.; Mazerant, W.; Meier, U. *Phys. Rev. B* **2000**, *61*, 10688.
(49) Meredith, G. R.; Buchalter, B. *J. Chem. Phys.* **1983**, *78*, 1938.
(50) Wortmann, R. *Habilitationsschrift*; Johannes Gutenberg Universität Mainz, Germany, 1993.
(51) Mountain, R. D. *J. Chem. Phys.* **1997**, *107*, 3921.
(52) Stähelin, M.; Moylan, C. R.; Burland, D. M.; Willets, A.; Rice, J. E.; Shelton, D. P.; Donley, E. A. *J. Chem. Phys.* **1993**, *98*, 5595.
(53) Willetts, A.; Rice, J. E. *J. Chem. Phys.* **1993**, *98*, 426.